Extreme Mechanics Letters 46 (2021) 101317

Contents lists available at ScienceDirect

Extreme Mechanics Letters

journal homepage: www.elsevier.com/locate/eml

Toughness of a composite in which sliding between fibers and matrix is rate-sensitive

Shawn R. Lavoie [a,1], Sammy Hassan [a,1], Junsoo Kim [a], Tenghao Yin [a,b], Zhigang Suo [a,*]

[a] John A. Paulson School of Engineering and Applied Sciences, Kavli Institute for Bionano Science and Technology, Harvard University, MA, 02138, USA

[b] State Key Laboratory of Fluid Power & Mechatronic System, Key Laboratory of Soft Machines and Smart Devices of Zhejiang Province, Center for X-Mechanics, and Department of Engineering Mechanics, Zhejiang University, Hangzhou 310027, China

ARTICLE INFO

Article history:
Received 18 February 2021
Received in revised form 5 April 2021
Accepted 6 April 2021
Available online 20 April 2021

Keywords:
Shear lag
Stress de-concentration
Fracture toughness
Sliding stress
Ceramic matrix composites

ABSTRACT

It has been common to use brittle constituents to form tough composites. For example, ceramic fibers and a ceramic matrix are brittle, but their composite can be tough, provided the matrix can slide relative to the fibers. Here we study the effect of rate-dependent sliding on toughness. Consider a crack through the matrix, with the fibers being intact and bridging the crack. The composite is subject to a tensile load normal to the crack. Both the fibers and the matrix are elastic, and the sliding stress between them is linear in their relative velocity. Far away from the crack, the matrix does not slide relative to the fibers, and the deformation is elastic. Near the crack, the matrix slides relative to the fibers, and the deformation is inelastic. When the rate of the applied load is low, the sliding stress is low, so that tension in each fiber is distributed over a long length. Breaking the fiber dissipates elastic energy over a long length of the fiber. This de-concentration of stress leads to high toughness. When the rate of the applied load is high, the sliding stress is also high, so that tension in the fiber is concentrated in a short length near the crack plane. This concentration of stress leads to low toughness. We model this rate-sensitive toughness using a shear lag model. The strain in the fiber satisfies a diffusion equation. When the composite is subjected to load at a constant strain rate, before the fiber breaks, the sliding zone increases with time. We discuss stress de-concentration in various materials.

1. Introduction

Brittle materials are all alike; every tough material is tough in its own way. Nonetheless some toughening mechanisms are more generally applicable than others. Perhaps the most generally appreciated toughening mechanism is inelasticity [1,2]. Examples include metals, plastics, and viscoelastic elastomers. This paper focuses on another general toughening mechanism, which is exemplified by a ceramic matrix composite. Ceramics are brittle, but a composite made of two ceramics can be tough [3]. Consider a composite made of a ceramic matrix and long, unidirectional ceramic fibers (Fig. 1). Both the matrix and fibers obey linear elasticity and have comparable elastic moduli. The matrix has large flaws, but the fibers have small diameters and therefore small flaws. Because of the large difference in flaw size, the matrix has low strength, and the fibers have high strength [4]. When the composite is subject to a tensile load, a crack may run through the matrix, but the fibers are intact. The interface between the matrix and the fibers is weak, so that the matrix debonds from the fibers and slides relative to the fibers. The sliding stress between the matrix and fibers is much smaller than the strength of the fibers, so that the length of the sliding zone is much larger than the radius of the fibers. Remote from the crack, the matrix and fibers remain bonded and deform by a homogeneous elastic strain. At the crack, the matrix is traction-free, and the fibers carry the entire load. As the distance along the fibers increases from the crack, the tensile stress in the fibers gradually and partially transfers to the matrix. This process of transferring tension by shear is called shear lag [5]. Unlike a crack in a homogeneous ceramic, the crack in the matrix does not concentrate stress to the atomic scale. Rather, the stress distributes along the fiber to a length much larger than the radius of the fiber. Breaking a single fiber releases elastic energy in a long segment of the fiber. This de-concentration of stress toughens the ceramic matrix composite. The lower the sliding stress, the longer the segment over which the elastic energy is stored, and the tougher the composite [6–8], (Marshall et al. 1985). Although the matrix is often necessary to hold the fibers together, if the matrix were not present, stress would deconcentrate along the entire length of the fibers, and the toughness would be enormous.

* Corresponding author.
E-mail address: suo@seas.harvard.edu (Z. Suo).
[1] These authors contributed equally to this work.

https://doi.org/10.1016/j.eml.2021.101317
2352-4316/

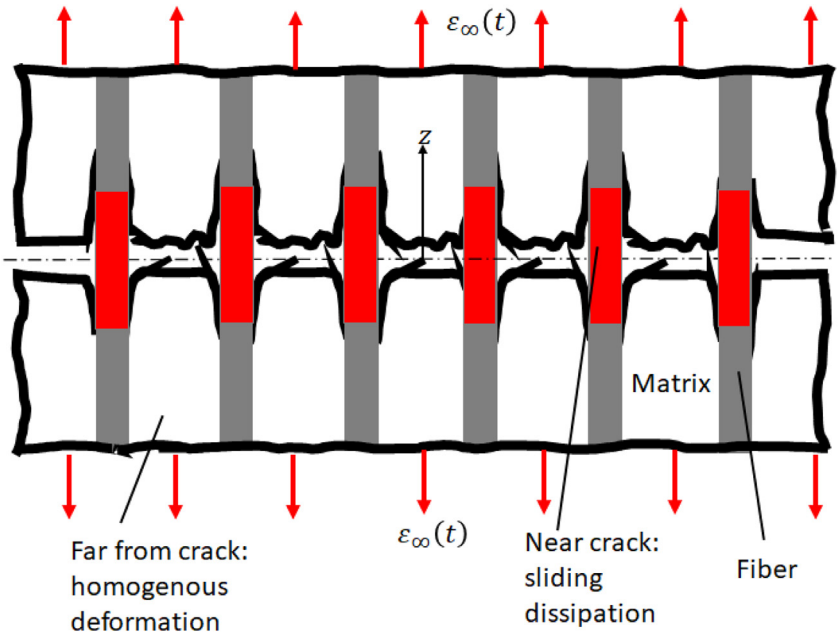

Fig. 1. A schematic of a composite in which a crack runs in the matrix, but the fibers are intact and bridge the crack. The fibers and the matrix are elastic. When the composite is subject to a time-dependent tensile load, the strain field far from the crack is time-dependent and homogeneous $\varepsilon_\infty(t)$, and there is no relative sliding between the matrix and the fiber. Near the crack, the fibers slide relative to the matrix. The length of the sliding zone increases with time. Breaking a fiber releases elastic energy stored in a long length of the fiber.

For example, glass is brittle, but a fabric of glass fibers is tough, in the absence of a polymer matrix.

The same mechanism operates in several classes of materials. In a fabric, the sliding stress between the fibers is much smaller than the strength of the fibers. Before a fiber breaks, the tension is distributed over a long length of the fiber. When the fiber breaks, the elastic energy in the long length of the fiber is released, amplifying toughness [9]. In a polymer network of a gel or an elastomer, the bonds in a polymer chain are covalent and strong, but the interactions between polymer chains are noncovalent and weak. Before a polymer chain breaks, the tension is distributed over a long length of the polymer chain. When the polymer chain breaks, the elastic energy in the long length of the polymer chain is released, amplifying toughness [10].

Whereas the weak interfacial interactions are known to toughen many classes of materials, their rate sensitivity on toughness is not well understood. The sliding stress can be rate-dependent [11–14]. Following [15,16], we formulate a shear lag model in which the sliding stress is linear in the sliding velocity (Section 2). We then use this model to analyze the effect of rate-dependent sliding on toughness. When the sliding stress increases with loading rate, the length over which stress de-concentrates shortens, and the material embrittles. To analyze the rate-embrittling effect in some detail, we focus on ceramic matrix composites. The strain in a fiber satisfies a diffusion equation. We apply the model to a composite subject to remote tension at a constant strain rate $\dot{\varepsilon}_\infty$ (Section 3). A self-similar solution exists, in which the length of the sliding zone is proportional to the square root of time. This model predicts that the toughness scales with the strain rate as $G_c \sim \dot{\varepsilon}_\infty^{-1/2}$ (Section 4). We discuss further stress de-concentration in various materials (Section 5).

2. Diffusive shear lag

Consider a unidirectional composite, in which fibers are periodically embedded in a matrix. In a cross section of the composite, we mark a unit cell for analysis (Fig. 2a). The cross section of a fiber is circular, radius R. Let c be the ratio of the volume of fibers to that of the composite. In the cross section of the unidirectional composite, c is also the area fraction of the fibers in the cross section of the composite. Let z be the distance along the fibers from the plane of the crack in the matrix (Fig. 1). Remote from the crack and in the direction of the fibers, the composite is subject to a homogeneous, time-dependent strain $\varepsilon_\infty(t)$. Near the crack, the matrix slides relative to the fibers, so that the strains in the fibers and matrix are different and vary along z, $\varepsilon_f(z,t)$ and $\varepsilon_m(z,t)$. The strains are related to the displacements in the fibers and matrix, $u_f(z,t)$ and $u_m(z,t)$, as usual

$$\varepsilon_f = \frac{\partial u_f(z,t)}{\partial z}, \qquad \varepsilon_m = \frac{\partial u_m(z,t)}{\partial z}. \tag{1}$$

The stresses in the fibers and matrix are also different and vary along z, $\sigma_f(z,t)$ and $\sigma_m(z,t)$. Let $\tau(z,t)$ be the sliding stress between the matrix and fiber. The balance of forces on an infinitesimal section of a fiber requires that (Fig. 2b)

$$\frac{\partial \sigma_f(z,t)}{\partial z} = -\frac{2}{R}\tau. \tag{2}$$

Define the average stress remote from the crack by $\sigma_\infty(t) = c\sigma_f(\infty,t) + (1-c)\sigma_m(\infty,t)$. The balance of forces on a section of the composite starting at position z and extending to the far field gives that (Fig. 2c)

$$\sigma_\infty(t) = c\sigma_f(z,t) + (1-c)\sigma_m(z,t). \tag{3}$$

Similarly, the balance of forces on a section of the composite starting at the crack plane and extending to the far field gives that (Fig. 2d)

$$\sigma_\infty(t) = c\sigma_f(0,t). \tag{4}$$

The fiber and matrix are linearly elastic:

$$\sigma_f = E_f\varepsilon_f, \qquad \sigma_m = E_m\varepsilon_m, \tag{5}$$

where E_f and E_m are Young's moduli of the fiber and matrix. Far from the crack, the composite is subject to a time-dependent load, represented by a homogeneous tensile strain field, $\varepsilon_f(\infty,t) = \varepsilon_m(\infty,t) = \varepsilon_\infty(t)$. The stress field is inhomogeneous because

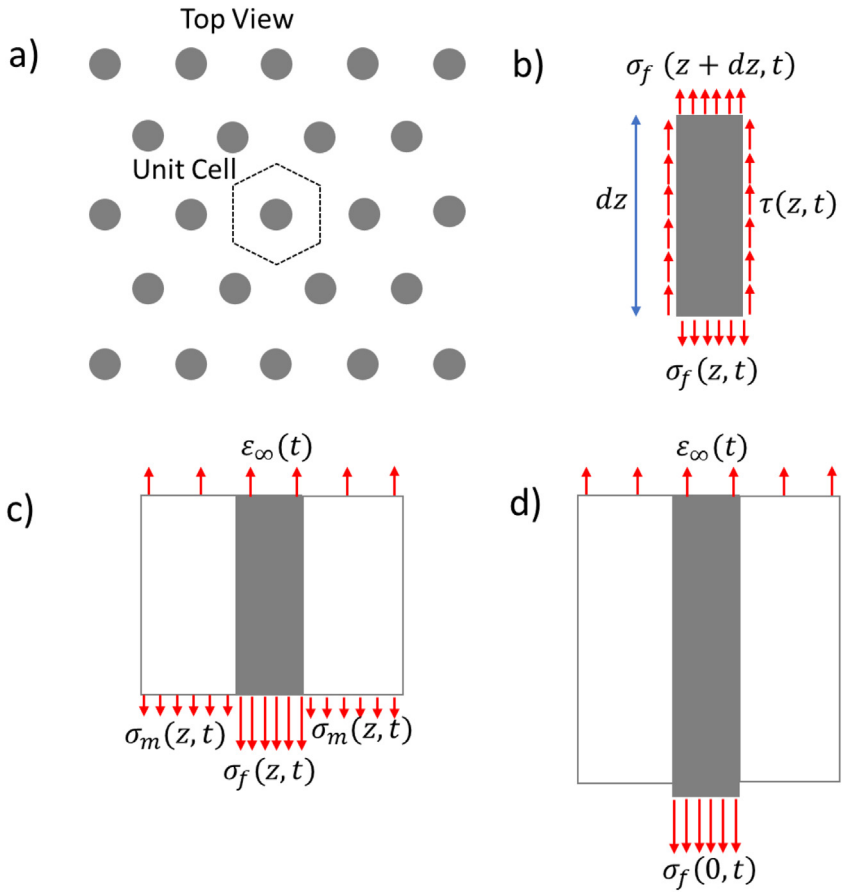

Fig. 2. A model of diffusive shear lag. (a) Marked in a cross section of the composite is a unit cell for analysis. (b) A free-body diagram of an infinitesimal section of the fiber of length dz. (c) A segment of the unit cell extending from an arbitrary position z to the far field. (d) A segment of the unit cell extending from the crack plane to the far field.

the matrix and the fiber have different moduli, so that $\sigma_f(\infty,t)=E_f\varepsilon_\infty(t)$ and $\sigma_m(\infty,t)=E_m\varepsilon_\infty(t)$. Thus, $\sigma_\infty(t)=E_l\varepsilon_\infty(t)$, where the effective modulus of the composite in the longitudinal direction is

$$E_l = cE_f + (1-c)E_m. \tag{6}$$

Note that E_l is also called the iso-strain effective modulus.

The shear stress τ is taken to be linear in the velocity of the matrix relative to the fiber:

$$\tau = \xi\frac{\partial\left(u_m-u_f\right)}{\partial t}, \tag{7}$$

where ξ is the viscous sliding coefficient. We neglect Poisson's effect and assume that the matrix and fiber remain in contact with the constant viscous sliding coefficient throughout the sliding. A combination of the above equations gives that

$$\frac{\partial\left(\varepsilon_f-\varepsilon_\infty\right)}{\partial t} = D\frac{\partial^2\left(\varepsilon_f-\varepsilon_\infty\right)}{\partial z^2}, \tag{8}$$

where

$$D=\frac{RE_t}{2c\xi}, \tag{9}$$

and

$$\frac{1}{E_t}=\frac{1}{cE_f}+\frac{1}{(1-c)E_m}. \tag{10}$$

Eq. (8) takes the form of a partial differential equation for one-dimensional diffusion, where D is the effective diffusivity. In the expression of D is the transverse equivalent modulus of the composite, E_t, defined by Eq. (10). Note that E_t takes the form of the effective stiffness of springs in series (i.e., iso-stress equivalent modulus). In shear lag, the tensile stress is transferred from the fiber to the matrix through the sliding stress. It is perhaps unsurprising that the iso-stress equivalent modulus appears in Eq. (9).

3. A composite subject to a constant strain rate

We solve the partial differential Eq. (8) under the following initial and boundary conditions. Before the far field strain is applied, the strain in the entire fiber is zero, $\varepsilon_f(z,0)=0$. Starting at time zero, the composite is subject to a homogeneous strain field, far from the crack, of constant rate $\dot{\varepsilon}_\infty$, so that $\varepsilon_f(\infty,t)=\dot{\varepsilon}_\infty t$. On the crack plane, the balance of forces Eq. (4) gives that $\varepsilon_f(0,t)=E_l\dot{\varepsilon}_\infty t/cE_f$. To remove time dependence from the boundary conditions, differentiate Eq. (8) and the boundary conditions with respect to time and formulate a boundary value problem for $\dot{\varepsilon}_f-\dot{\varepsilon}_\infty$. Thus, we can write the following initial condition:

$$\dot{\varepsilon}_f(z,0)-\dot{\varepsilon}_\infty=0. \tag{11}$$

Next, consider the boundary conditions of the composite. At $z=\infty$, there is no relative motion between the matrix and the fiber. Therefore, the strain rate in the fiber is the same as that applied in the far field:

$$\dot{\varepsilon}_f(\infty,t)-\dot{\varepsilon}_\infty=0. \tag{12}$$

Since $z=0$ represents the crack surface, the matrix it is stress free $\sigma_m(z=0,t)=0$; therefore $\dot{\varepsilon}_f(z=0,t)$ can be obtained

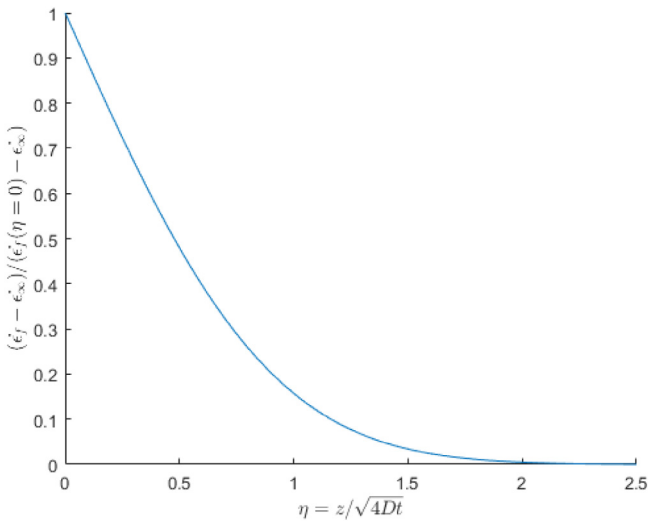

Fig. 3. Normalized strain rate as a function of the similarity variable.

from Eq. (4)

$$\dot{\varepsilon}_f(0,t) - \dot{\varepsilon}_\infty = \frac{(1-c)E_m}{cE_f}\dot{\varepsilon}_\infty. \tag{13}$$

Eqs. (8) and (11)–(13) represent a classical diffusion boundary value problem for $\dot{\varepsilon}_f(z,t) - \dot{\varepsilon}_\infty$, for which a solution is obtained by introducing the following similarity variable:

$$\eta = \frac{z}{\sqrt{4Dt}}, \tag{14}$$

which transforms Eq. (8) into an ordinary differential equation. The solution is,

$$\dot{\varepsilon}_f(z,t) - \dot{\varepsilon}_\infty = \frac{(1-c)E_m}{cE_f}\dot{\varepsilon}_\infty(1 - erf\,\eta). \tag{15}$$

The normalized result of Eq. (15) is shown in Fig. 3. At $\eta = 0$, which represents $z = 0$ or $t = \infty$, the value of the function is 1. The function is monotonically decreasing and vanishes as $\eta \to \infty$, which represents $z \to \infty$ or $t = 0$.

Integrating Eq. (15) with respect to time and noting that $\varepsilon_f(z, t=0) = 0$ gives

$$\varepsilon_f(z,t) = \frac{(1-c)E_m}{cE_f}\dot{\varepsilon}_\infty t\left(\left(1+2\eta^2\right)(1-erf\,\eta) - 2\eta\frac{e^{-\eta^2}}{\sqrt{\pi}}\right) + \dot{\varepsilon}_\infty t. \tag{16}$$

The strain in the fiber is plotted against the normalized position (z/R) for a fixed strain rate (Fig. 4a). The strain profiles evolve with time. Initially there is no strain in the fiber. As time progresses not only does ε_∞ increase, but a strain-concentration forms at $z = 0$ and expands along the length of the fiber. Eq. (16) also illustrates how larger strain rates can concentrate strain within the fiber (Fig. 4b). All of the curves have the far field strain $\varepsilon_\infty = \dot{\varepsilon}_\infty t$ held constant.

Using Eq. (14), we find that sliding takes place in a zone of length scaling as $l \sim \sqrt{4Dt}$. As time progresses the length of the sliding zone increases. Assume that the fiber breaks when a specified strain, ε_b, is reached. The maximum strain in the fiber occurs at $z = 0$. We can determine the far field strain at which failure occurs using Eq. (4) and obtain

$$t_b = \frac{cE_f\varepsilon_b}{E_l\dot{\varepsilon}_\infty}. \tag{17}$$

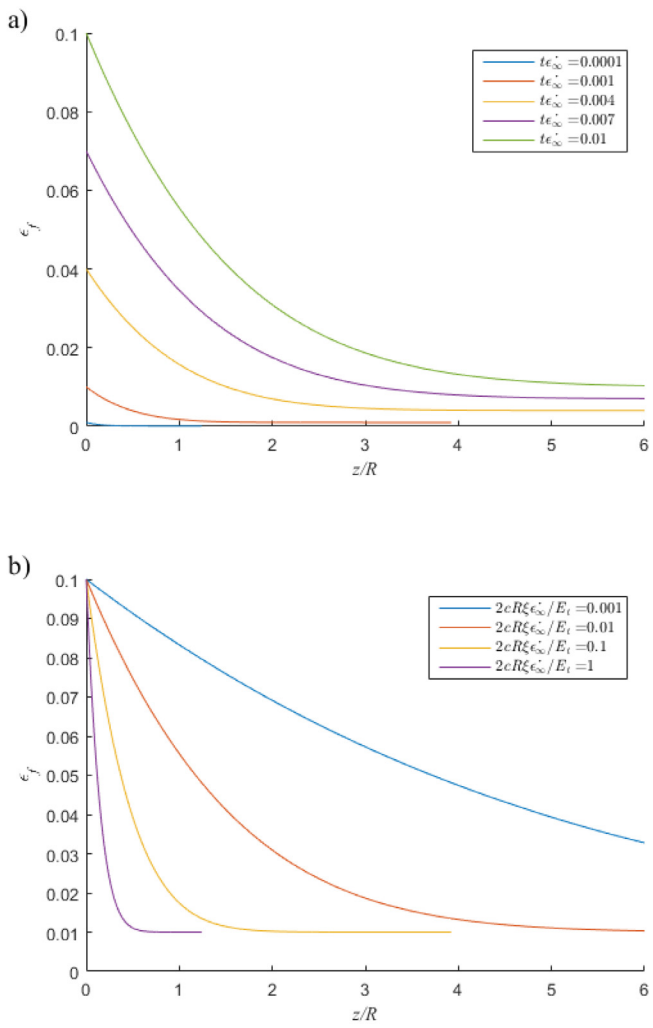

Fig. 4. (a) The distribution of strain in the fiber at several times. As time advances, the far field strain increases and the strain becomes concentrated near the crack tip. The concentrated region propagates farther along the fiber as time advances. Here the normalized strain rate is held fixed $2cR\xi\dot{\varepsilon}_\infty/E_t = 0.01$. (b) The strain in the fiber vs the normalized position for a fixed far field strain ε_∞. The lower asymptote of the vertical axis represents ε_∞. Each curve represents a different normalized far field strain rate. For all curves $c = 0.1$ and $E_f/E_m = 1$.

Given this time scale, we can scale the length of the slip zone at break $l_b \sim \sqrt{4Dt_b}$, which after substitution and simplification gives:

$$l_b \sim \sqrt{\frac{2RE_fE_t\varepsilon_b}{E_l\xi\dot{\varepsilon}_\infty}}. \tag{18}$$

4. Rate-sensitive toughness and fracture cohesive length

We define the crack bridging model in the following context. The background material is an elastic composite in which fibers do not slide relative to the matrix. Relative to the background material there is excess displacement due to the sliding between fibers and the matrix. Following [17], we define the crack opening displacement as the excess displacement relative to the elastic displacement of a composite where the matrix and the fiber are perfectly bonded and have homogeneous strain:

$$\delta(t) = \lim_{z\to\infty} 2\left(u_f(z,t) - \varepsilon_\infty(t)z\right). \tag{19}$$

We obtain $u_f(z,t)$ using the solution in Section 3 and the boundary condition $u_f(z=0,t)=0$. The crack opening displacement increases with time as

$$\delta(t) = R\frac{8(1-c)E_m}{3\sqrt{\pi}cE_f}\sqrt{\frac{E_t}{2c\xi\dot{\varepsilon}_\infty R}}(\dot{\varepsilon}_\infty t)^{\frac{3}{2}}. \tag{20}$$

In the crack bridging model, the stress in the composite far away from the crack plane defines the traction, $\sigma_\infty = E_l\varepsilon_\infty$. Eq. (20) shows that the traction–separation relation scales as $\delta \sim \sigma_\infty^{3/2}$. We plot the normalized traction–separation curves for various non-dimensional strain rates (Fig. 5). For higher strain rates, the traction rises more quickly with the crack opening. Let us specify a breaking strain for the fiber, ε_b. The far field strain at failure is $(\varepsilon_\infty)_b = c\varepsilon_b$, corresponding to a horizontal line in Fig. 5. The area under the traction–separation curves, up to the breaking traction, is the excess work done by the far field stress due to the sliding between the matrix and the fiber. This excess work is the toughness of the composite:

$$G_c = \int_0^{\delta_b=\delta(t_b)} \sigma_\infty d\delta, \tag{21}$$

where δ_b is the crack opening when the fiber breaks. From Fig. 5 we see that for a given breaking strain, ε_b, a higher applied strain rate will result in a less area under the traction–separation curve and a lower toughness. The integration gives that

$$G_c = \frac{8E_t}{5}\sqrt{\frac{RE_fE_t}{2\pi E_l\xi\dot{\varepsilon}_\infty}}\varepsilon_b^{5/2}. \tag{22}$$

Note that $G_c \sim \dot{\varepsilon}_\infty^{-0.5}$ and $G_c \sim \xi^{-0.5}$. For a constant E_l smaller values of c and E_m/E_f would produce the highest values of G_c. Introducing the slip length Eq. (18) into Eq. (22) and dropping all constants we get the following scaling relationship

$$G_c \sim l_bE_t\varepsilon_b^2. \tag{23}$$

Note that $E_t\varepsilon_b^2$ has the dimensions of strain energy density so G_c scales with the product of the strain energy density and the slip length. In the Appendix we derive the contributions to G_c from sliding dissipation and the release of stored elastic energy. These components are found to have about the same magnitude.

5. Stress de-concentration in various materials

Toughness is measured using a material containing a precut crack. Imagine a composite containing a precut crack through both the matrix and the fibers. To simplify the discussion, assume that the matrix and fibers have an identical modulus. First consider the case where the matrix and the fibers are perfectly bonded and do not slide relative to each other. Consequently, the composite is indistinguishable from a homogeneous, elastic material. When the material is stretched, the stress at the crack tip concentrates all the way to the atomic scale [4]. For this homogeneous elastic material, the toughness is the covalent energy of a single layer of atomic bonds, $G_c \sim bJ/V$, where b is the size of an atom, J is the energy to rupture an atomic bond, and V is the volume per bond.

It is the stress concentration that makes a homogeneous elastic material brittle. Many synthetic and natural materials acquire high toughness through mechanisms of stress de-concentration. In what follows we recall several examples. In all these examples rate sensitivity can be important, but to simply the description we do not discuss rate effects.

In the body of this paper, we assume that the matrix slides relative to the fibers. Consider a fiber at the crack tip. Before the fiber breaks, the high stress is distributed over a long length in the fiber, comparable to the sliding zone length. Consequently, the toughness scales as $G_c \sim l_bW_b$, where l_b is the sliding zone length, and W_b is the elastic energy per unit volume in the fiber at breaking. Thin fibers approach the theoretical strength of a material, so that W_b is comparable to J/V. However, l_b is enormous compared with b. In the composite, the relative sliding between the fibers and the matrix de-concentrates stress. It is this stress de-concentration that amplifies toughness. It is well-known that the fiber/matrix interfaces in a ceramic matrix composite can become viscous at high temperatures [11–13]. However, we have not seen the measurement of toughness of such composites as a function of rates. We have recently observed the key attributes described in this paper in a hydrogel. The stress–strain curves of the hydrogel are rate insensitive, but the toughness of the hydrogel decreases as the rate increases. We will report this experimental observation in a separate paper.

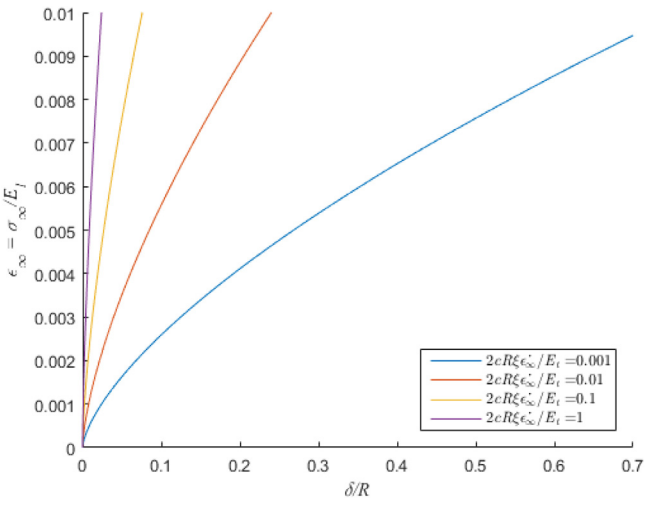

Fig. 5. Dimensionless traction displacement curves for various values of applied normalized strain rate ($2c\xi\dot{\varepsilon}_\infty R/E_t$). The upper limit of the stress axis represents the point at which the fiber breaks. The area enclosed by this curve is representative of the fracture toughness. Hence as the far field strain rate is increased the stress rises more quickly and the results in lower fracture energy. The breaking strain $(\varepsilon_\infty)_b$ corresponds to a horizontal line.

Stress-deconcentration also occurs in elastomers and gels. Such a material has a network of polymer chains. The bonds along each chain are covalent and strong, while the interactions between chains are noncovalent and weak. The toughness of the network is understood in terms of the Lake–Thomas model [10]. Consider a polymer chain at the crack tip. Before the chain breaks, the weak interchain interactions enable the chain to slide relative to other chains, so that high stress is distributed along the entire length of the chain. Consequently, the toughness is the covalent energy per unit area of a layer of polymer chains, $G_c \sim l_cJ/V$. Here $l_c = b\sqrt{m}$ is the end-to-end distance of the polymer chain, where b is the length of a monomer, and m is the number of monomers per chain. The weak interchain interactions de-concentrates stress over the length of the polymer chain and toughens the network.

In this paper, we have focused on a specific toughening mechanism. However, polymeric materials are known to have many other toughening mechanisms as illustrated in the following examples. Viscoelasticity will cause a dissipation zone in the bulk material around the crack tip and toughens the material [18]. In rubbery un-crosslinked polymers, the chains can pull out without breaking, which gives a different rate dependence of toughness [19]. In some glassy polymers, the interchain interactions are significant compared to the forces along chain, so that the chains

break before the stress is de-concentrated along long length [20]. In many elastomers and hydrogels, stochasticity of polymer networks causes chains to rupture away from the crack tip [21]. In a double-network elastomer and hydrogel, the short-chain network ruptures first away from the crack and the long-chain network remains intact [22,23]. The diversity of toughening mechanisms in polymeric materials causes various responses of toughness to strain rate. Within the model that couples bridging and background dissipation, one may regard our mechanism as crack bridging. Recall that a small change in bridging can be greatly amplified by background dissipation [24]. However, a study of how these mechanisms couple in polymeric materials is beyond the scope of this paper.

The same stress de-concentration also applies in a lattice material. In a lattice, the only interactions between members are at joints. If the joints are pinned, as in a truss, then each member can carry only tensile or compressive forces, and the entire member has a constant stress along its length. Consequently, the toughness of lattice scales with the breaking energy of a layer of members per unit area [25].

Stress can also be de-concentrated in composites with strong interfacial bonding but with a large difference in the elastic moduli of the fibers and the matrix. For instance, in a polymer matrix composite, fibers (e.g., carbon or glass) are much stiffer than the matrix, and fibers and the matrix are well-bonded. Consider a fiber at the crack tip. When the composite is stretched, the compliant matrix shears easily, so that high stress is distributed over a long length of the fiber [5]. This stress de-concentration toughens the composite [26].

The same principle has guided the recent development of composites in which both matrix and fiber are stretchable [27,28]. In such a stretchable composite, the matrix and the fibers have high contrast in elastic moduli and are well-bonded. Consider a fiber at the crack tip. The high contrast in elastic moduli de-concentrates stress along the length of the fiber via matrix shearing. This stress de-concentration toughens the composite. Furthermore, in a stretchable composite, the stiff phase need not be in the form of fibers, but can be in any arrangement, such as a lattice [29].

The principle of stress concentration also applies to biological materials. For example, in nacre, mineral platelets and protein form a brick–mortar structure. Consider a mineral platelet at a crack tip. When the nacre is stretched, the protein layer shears substantially, and high tension is distributed over the entire length of the platelet [30,31]. This stress de-concentration makes the nacre much tougher than the mineral. This principle has been used to guide the recent development of nacre like composites [32,33].

6. Conclusion

We studied the effect of loading rate on the toughness of a composite, in which the matrix slides relative to fibers. The sliding stress is taken to be linear in the sliding velocity. Consider a crack running through the matrix with all the fibers intact and bridging the crack. When the composite is stretched, the matrix slides relative to the fibers. The sliding stress transfers tension from the matrix to the fibers. When the sliding stress is low, high tension is distributed over a long length of the fibers. This stress de-concentration toughens the composite. At higher loading rates, sliding stress increases and retards the sliding between the matrix and the fibers. The sliding zone becomes smaller and tension is disturbed over a short length. Consequently, high loading rates embrittle the composite. We further discuss toughening by stress de-concentration in several synthetic and natural materials. It is hoped that this paper will aid the design of tough materials.

Nomenclature

b	Size of an atom or monomer
c	Ratio of the volume of fibers to that of the composite
D	Effective diffusivity
$\delta\,(t)$	Crack opening displacement
E_f	Young's modulus of fiber
E_m	Young's modulus of matrix
E_l	Effective composite modulus in longitudinal direction
E_t	Effective composite modulus in transverse direction
$\varepsilon_f\,(z,t)$	Strain in the fiber
$\varepsilon_m\,(z,t)$	Strain in the matrix
$\dot{\varepsilon}_\infty$	Far field strain rate
$\varepsilon_\infty\,(t)$	Far field strain
$(\boldsymbol{\varepsilon}_\infty)_{\boldsymbol{b}}$	Far field strain for fiber break
ε_b	Strain at which fiber breaks
η	Similarity variable
G_c	Toughness
J	Energy to rupture an atomic bond
l	Scaling length of zone of sliding
l_b	Scaling length of zone of sliding at fiber break
l_c	end-to-end distance of the polymer chain
m	the number of monomers per chain
ξ	Viscous friction coefficient
R	Radius of fiber
σ_f	Stress in fiber
σ_m	Stress in matrix
$\sigma_\infty\,(t)$	Far field average stress
t	time
t_b	Time at which fiber breaks
τ	Shear stress between matrix and fiber
u_f	Fiber displacement
u_m	Matrix displacement
v	Volume of a bond
W_b	elastic energy per unit volume in the fiber at breaking
z	Distance along the fibers from the plane of the crack

Declaration of competing interest

The authors declare that they have no known competing financial interests or personal relationships that could have appeared to influence the work reported in this paper.

Acknowledgments

This work is supported by Air Force Office of Scientific Research, USA under award number FA9550-20-1-0397. S.R.L acknowledges financial support from the Natural Science and Engineering Research Council (NSERC), Canada.

Appendix. Energy dissipation

Consider conservation of energy per unit area of the composite. The work applied, W, is either stored as elastic energy, U, or dissipated as heat, Φ:

$$W = U + \Phi. \tag{A.1}$$

Note that W and U are infinite in our model, but Φ is finite. The work is given by

$$W = 2\int_0^{u_\infty} \sigma_\infty du_\infty. \tag{A.2}$$

where u_∞ is the far field displacement. That factor 2 accounts for the contributions from both sides of the crack. The stored elastic energy consists of contributions from both the matrix and the fibers:

$$U = 2\int_0^\infty cE_f\frac{\varepsilon_f^2}{2} + (1-c)\,E_m\frac{\varepsilon_m^2}{2}dz. \tag{A.3}$$

The dissipation is the work done by the sliding stress τ, in the entire sliding zone:

$$\Phi = \frac{4\xi c}{R}\int_0^\infty\int_0^{t_b} v_r^2 dtdz. \tag{A.4}$$

Consider an ideal composite with no sliding, so that the deformation in the matrix and the fibers is uniform. The elastic energy stored in the composite is:

$$U_{id} = 2\int_0^\infty E_l\frac{\varepsilon_\infty^2}{2}dz. \tag{A.5}$$

The toughness is the work done to the composite in excess of the energy stored in the ideal composite, $G_c = W - U_{id}$. Thus:

$$G_c = U - U_{id} + \Phi. \tag{A.6}$$

Note that U and U_{id} are both infinite in our model, but their difference is finite:

$$U - U_{id} = 2\int_0^\infty cE_f\frac{\left(\varepsilon_f^2 - \varepsilon_\infty^2\right)}{2} + (1-c)\,E_m\frac{\varepsilon_m^2 - \varepsilon_\infty^2}{2}dz. \tag{A.7}$$

Using Eqs. (A.4) and (A.7) we can evaluate the relative contributions to G from dissipation and unrecoverable elastic energy. We get $U - U_{id} = 0.4477G_c$, and $\Phi = 0.5523G_c$. Note that these results are independent of c, E_m, E_f, ε_b, and the nondimensional strain rate. This can be seen by substituting v_r^2, ε_f^2, and ε_m^2 into Eqs. (A.4), (A.7). After rearranging and grouping non-dimensional variables in Eqs. (A.4), (A.7) and Eq. (22) in the main text, we get

$$\frac{G}{RE_t} = \frac{8}{5\sqrt{\pi}}\varepsilon_b^{5/2}\sqrt{\frac{c}{c+(1-c)\,E_m/E_f}}\sqrt{\frac{E_t}{2c\xi\dot{\varepsilon}_\infty R}} \tag{A.8}$$

$$\frac{U-U_{id}}{RE_t} = 32\varepsilon_b^{5/2}\sqrt{\frac{c}{c+(1-c)\,E_m/E_f}}\sqrt{\frac{E_t}{2c\xi\dot{\varepsilon}_\infty R}} \times\int_0^\infty\left(\frac{\eta^2}{2}(1-\mathrm{erf}\eta) + \frac{1-\mathrm{erf}\eta}{4} - \frac{\eta e^{-\eta^2}}{2\sqrt{\pi}}\right)^2 d\eta \tag{A.9}$$

$$\frac{\Phi}{RE_t} = 32\varepsilon_b^{5/2}\sqrt{\frac{c}{c+(1-c)\,E_m/E_f}}\sqrt{\frac{E_t}{2c\xi\dot{\varepsilon}_\infty R}}\int_0^\infty \times\int_0^1\left(\frac{t}{t_b}\right)\left(\eta(1-\mathrm{erf}\eta) - \frac{e^{-\eta^2}}{\sqrt{\pi}}\right)^2 d\left(\frac{t}{t_b}\right)d\eta \tag{A.10}$$

In each equation, the integration is independent of the parameters of the model. The parameters appear in the coefficients of the integrals in the same way. Hence $(U-U_{id})/G_c$ and Φ/G_c are constants in this model.

References

[1] G.R. Irwin, Fracture dynamics, in: Fracturing metals, ASM Symposium (Tans. ASM 40A), Cleveland, 1948, pp. 147–166.
[2] E. Orowan, Fracture and strength of solids, Rep. Progr. Phys. 12 (1948) 185–232.
[3] A.G. Evans, Perspective on the development of high-toughness ceramics, J. Am. Ceram. Soc. 73 (1990) 187–206.
[4] A.A. Griffith VI, The phenomena of rupture and flow in solids, in: Series A, Containing Papers of a Mathematical or Physical Character, Philos. Trans. R. Soc. Lond. 221 (1921) 163–198.
[5] H.L. Cox, The elasticity and strength of paper and other fibrous materials, Br. J. Appl. Phys. 3 (1952) 72–79.
[6] A.H. Cottrell, Strong solids, Proc. R. Soc. Lond. Ser. A Math. Phys. Eng. Sci. 282 (1964) 2–9.
[7] B. Budiansky, J.W. Hutchinson, A.G. Evans, Matrix fracture in fiber-reinforced ceramics, J. Mech. Phys. Solids 34 (1986) 167–189.
[8] A.G. Evans, R.M. McMeeking, On the toughening of ceramics by strong reinforcements, Acta Metal. 34 (1986) 2435–2441.
[9] N.A. Teixeira, M.M. Platt, W.J. Hamburger, Mechanics of elastic performance of textile materials: Part XII: Relation of certain geometric factors to the tear strength of woven fabrics, Textile Res. J. 25 (1955) 838–861.
[10] G.J. Lake, A.G. Thomas, The strength of highly elastic materials, Proc. R. Soc. Lond. A 300 (1967) 108–119.
[11] S.V. Nair, K. Jakus, C. Ostertag, Role of glassy interfaces in high temperature crack growth in SiC fiber reinforced alumina, ceramic, Eng. Sci. Proc. 9 (1988) 681–686.
[12] R. Chaim, L. Baum, D. Brandon, Mechanical properties and microstructure of Whisker-reinforced alumina-30 vol% glass matrix composite, J. Am. Ceram. Soc. 72 (1989) 1636–1642.
[13] H. Kodama, H. Sakamoto, T. Miyoshi, Silicon carbide monofilament-reinforced silicon nitride or silicon carbide matrix composites, J. Am. Ceram. Soc. 72 (1989) 551–558.
[14] A. Ghatak, K. Vorvolakos, H. She, D.L. Malotky, M.K. Chaudhury, Interfacial rate processes in adhesion and friction, J. Phys. Chem. B. 104 (2000) 4018–4030.
[15] S.V. Nair, K. Jakus, T.J. Lardner, The mechanics of matrix cracking in fiber reinforced ceramic composites contain a viscous interface, Mech. Mater. 12 (1991) 229–244.
[16] C.H. Hsueh, Interfacial debonding and fiber pull-out stresses of fiber reinforced composites Part V. With viscous interface, Mater. Sci. Eng. A 149 (1991) 1–9.
[17] J.W. Hutchinson, H.M. Jensen, Models of fiber debonding and pullout in brittle composites with friction, Mech. Mater. 9 (1990) 139–163.
[18] A.N. Gent, Adhesion and strength of viscoelastic solids. Is there a relationship between adhesion and bulk properties? Langmuir 12 (1996) 4492–4496.
[19] T. Baumberger, C. Caroli, D. Martina, Solvent control of crack dynamics in a reversible hydrogel, Nature Mater. 5 (2006) 552–555.
[20] J. Washiyama, E.J. Kramer, C.F. Creton, C-.H. Hui, Chain pullout fracture of polymer interfaces, Macromolecules 27 (1994) 2019–2024.
[21] J. Slootman, V. Waltz, J. Yeh, C. Baumann, R. Göstl, J. Comtet, C. Creton, Quantifying rate- and temperature-dependent molecular damage in elastomer fracture, Phys. Rev. X 10 (2020) 041045.
[22] J.P. Gong, Y. Katsuyama, T. Kurokawa, Y. Osada, Double-network hydrogels with extremely high mechanical strength, Adv. Mater. 15 (2003) 1155–1158.
[23] E. Ducrot, Y. Chen, M. Bulters, R.P. Sijbesma, C. Creton, Toughening elastomers with sacrificial bonds and watching them break, Science 344 (2014) 186–189.
[24] V. Tvergaard, J.W. Hutchinson, The relation between crack growth resistance and fracture process parameters in elastic–plastic solids, J. Mech. Phys. Solids 40 (1992) 1377–1397.
[25] N.E.R. Romijn, N.A. Fleck, The fracture toughness of planar lattices: imperfection sensitivity, J. Mech. Phys. Solids 55 (2007) 2538–2564.
[26] C.Y. Hui, Z. Liu, S.L. Phoenix, Size effect on elastic stress concentrations in unidirectional fiber reinforced soft composites, Extreme. Mech. Lett. 33 (2019) 100573.
[27] Z. Wang, C. Xiang, X. Yao, P. Le Floch, J. Mendez, Z. Suo, Stretchable materials of high toughness and low hysteresis, Proc. Natl. Acad. Sci. USA 116 (2019) 5967–5972.
[28] C. Xiang, Z. Wang, C.H. Yang, X. Yao, Y. Wang, Z. Suo, Stretchable and fatigue-resistant materials, Mater. Today 34 (2020) 7–16.
[29] C. Li, H. Yang, Z. Suo, J. Tang, Fatigue-resistant elastomers, J. Mech. Phys. Solids 134 (2020) 103751.
[30] R.Z. Wang, Z. Suo, A.G. Evans, N. Yao, I.A. Aksay, Deformation mechanisms in nacre, J. Mater. Res. 16 (2001) 2485–2493.
[31] H. Gao, B. Ji, I.L. Jäger, E. Arzt, P. Fratzl, Materials become insensitive to flaws at nanoscale: Lessons from nature, Proc. Natl. Acad. Sci. USA 100 (2003) 5597–5600.
[32] R.O. Ritchie, The conflicts between strength and toughness, Nature Mater. 24 (2011) 817–822.
[33] Z. Yin, F. Hannard, F. Barthelat, Impact resistant nacre-like transparent materials, Science 364 (2019) 1260–1263.